OPEN ACCESS

Saudi Journal of Engineering and Technology
Abbreviated Key Title: Saudi J Eng Technol
ISSN 2415-6272 (Print) | ISSN 2415-6264 (Online)
Scholars Middle East Publishers, Dubai, United Arab Emirates
Journal homepage: https://saudijournals.com

Original Research Article

Analysis of Entropy Generation for MHD Heat Transfer Flow of Viscous Fluid Embedded in a Porous Channel Due to Thermal Radiation

Ibrahim Ahmad, S[1*], Aisha A. Haliru[2], Ibrahim D. Yale[3], Zayyanu, S. Y[4]

[1]Department of Mathematics, Faculty of Physical Sciences, Kebbi State University of Science and Technology Aliero, Kebbi, Nigeria
[2]Department of Mathematics, Faculty of Science, Bayero University, Kano, Nigeria
[3]Department of Mathematics, Faculty of Physical Sciences, Kebbi State University of Science and Technology Aliero, Kebbi, Nigeria
[4]Department of Mathematics, Faculty of Science, Sokoto State University, Sokoto, Nigeria

DOI: 10.36348/sjet.2024.v09i02.010 | **Received:** 08.01.2024 | **Accepted:** 19.02.2024 | **Published:** 24.02.2024

***Corresponding author:** Ibrahim Ahmad, S
Department of Mathematics, Faculty of Physical Sciences, Kebbi State University of Science and Technology Aliero, Kebbi, Nigeria

Abstract

The study investigates the effect of convective flow on entropy generation for MHD heat transfer flow of viscous fluid embedded in a porous channel due to thermal radiation. The governing equations were transformed using the non-dimensional parameters. The solution of the resulting coupled dimensionless differential equations with a constant coefficient describing the momentum, energy, and mass transfer equations was obtained by using the method of undetermine coefficient. The parameters embedded in the flow are thermal radiation (N_r), Prandtl number, entropy generation (N_s), Suction/injection parameter (S), heat source/sink (Ks), porous material (K). In addition, physical quantities of engineering interest such as the Bejan number (Be), Brinkman number $\left(\frac{B_r}{\Pi}\right)$, volumetric flow rate (m), skin friction (τ) coefficient, and heat transfer rate (Q) were computed. It is noticed that velocity and temperature increase significantly with an increase in heat source and suction parameters, while a reverse trend is observed when heat sink and injection are present. It is also evident that, the heat source increases the temperature profile in the presence of injection parameter, and a reverse trend is observed when the heat sink increases in the presence of the suction parameter. skin friction is decreasing with increase higher values of porous material in both at $(\tau_{0,}\tau_1)$ when injection $(S=1)$ and $(\zeta=-1)$, volume flow rate reduces with increasing values of heat source and shot-up with decreasing values of heat sink, its observed that entropy generation is increasing for higher values of $\frac{B_r}{\Pi}$ when $(Ks=0)$.

Keywords: Entropy generation, Heat Source/Sink, MHD, Volume flow rate, Nusselt number.

1.0 INTRODUCTION

Natural convection heat transfer takes place both by thermal diffusion, the random motion of fluid molecules, and by advection, in which heat (matter) is transported by the larger-scale motion of current in the fluid. The mechanism that happens when a fluid, liquid, or gas is heated by flow occurs by a natural means called the buoyancy effect, which is density variation in the fluid. The convection heat transfer is usually subdivided into free and forced convection, and the fluid is blown or pumped past the heated surface using a fan. Barmert and Kupitz (1991) stated that, as the World Energy Council has noted, energy supplies will have to increase in the years ahead, especially in the electric sector, as well as thermal radiation usage, to meet the needs of the world's growing population. Worldwide About 30% of total primary energy (heat) is used to produce electricity, while most of the remaining 70% is either used in transportation or converted into hot water, steam, and heat. Heat source: the sun (solar energy); it's the biggest source of heat energy underground in vents and volcanoes as a result of chemical reactions inside battery cells, friction created when two objects rub against each other, Heat conduction with a heat source in rocks originates from the natural radioactivity of rocks, which produces heat. A heat sink is a component that increases the heat flow away from a hot device. It's like a coolant installed inside a system to move away or conduct heat generated by electronics appliances in order to degenerate or regulate temperature levels to enhance efficient work. A heat sink is designed to maximize its surface area in contact with the cooling medium surrounding it, such as air velocity, and the material involves passive heat sinks, which do not have a fan, while active heat sinks dissipate heated substances from the device by using fans such as ram modules, power transistors, optoelectronic light-emitting diodes, and chipsets for allowing normality of the device temperature.

Thermal radiation is the transfer of thermal energy by waves that travel through air or even empty space. Thermal radiation occurs in combination with conduction and convection and is significant where a large temperature difference occurs as a result of electromagnetic radiation. The ultraviolet, known as black light, visible, infrared, and microwave decay of uranium produces alpha-particles. Thermal energy is the energy possessed within an object or system; it often involves solids, liquids, and gases.

MHD means magnetohydrodynamics, magneto-fluid dynamics, or hydromagnetic. It is the study of the dynamics or motion of an electrically conducting fluid such as ionized gas or liquid metal interacting with a magnetic field the presented the concept of MHD, which is the most crucial aspect of inducing current in a moving conductive fluid. The magnetic properties of electrically conducting fluids such as magneto-fluid plasma, liquid metal, salt water, and electrolytes. Hunegnaw *et al.,* (2014) discovered that the effect of viscous dissipation leads to increased temperature profiles in cases of the presence or absence of a heat source or sink parameter. Due to the internal heat sink (0) the thermal boundary layer increases while decreasing with the heat source (0). Kumar and Singh (2014) and Taiwo *et al*., (2020) carried out an investigation on the effect of natural convective flow in an annulus with isothermal and isoflux boundaries with heat source/sink MHD. It was generally revealed that an increase in the heat source/sink parameter in turn, prompts an increase in the fluid velocity-induced magnetic field, and a fluid temperature-reversed trend is observed with a heat sink.

Entropy is the measure of the movement of a molecular disorder or the randomness of a system. The entropy generation produced an irreversible process of system thermal energy per unit temperature. The measurement of the magnitude of irreversibility present during entropy generation is encountered in energy-related applications such as solar power collectors, geothermal energy, and the cooling of modern electronics. Therefore, analysis of entropy generation is the technique of identification and reduction of thermodynamic irreversibility. Tasnim *et al., (2002)* described analytically the influence of entropy generation in porous mediums under the effect of hydromagnetic. He concluded that higher entropy generation is achieved near the wall of the channel. Mahmud (2005) examined heat and mass flow on the entropy generation characteristic effect inside a porous channel with viscous dissipation. The effect of an externally oriented magnetic field on entropy generation in natural convection has been reported by Jerry *et al.*, (2010). Chauhan and Kumar (2011) studied heat transfer and entropy generation during compressible fluid flow in a channel partially filled with porous medium. Sanatan and Rabindra (2013) studied the entropy generation in MHD flow through a porous channel under a constant pressure gradient. It is shown that entropy generation decreases with an increase in the magnetic field parameter.

2.0 MATHEMATICAL FORMULATION OF THE PROBLEM

Think about a magnetic field and a steady flow of a viscous fluid that conducts electricity through a channel made of two porous plates. This flow can't be slowed down. The flow is assumed to be in the x-axis parallel to the force of gravity g, but in the opposite direction it is separated by length b. The y-axis is normal to the vertical parallel channel. Initially let $(0, B_{0,}, 0)$ be the uniform strength of the magnetic field, which is implemented in the y direction. The influence of the induced magnetic field can be neglected by letting the very low magnetic Reynold's assumption. The temperature of one plate of the vertical channel is fixed at T_1, while the other plate is maintained at a constant temperature T_2 with $T_1 > T_2$ within the framework of the above-stated assumption, the mass, momentum, and energy balance equations with thermal radiation are formulated as follows: the governing equations for the analysis of entropy generation for thermal radiation MHD flow in a vertical porous channel due to heat source or sink.

Mass Equation

$$\frac{\partial u}{\partial t} = o \quad \ldots\ldots\ldots\ldots\ldots\ldots\ldots\ldots\ldots\ldots\ldots \text{(3.1)}$$

Momentum Equation

$$v\frac{\partial^2 u}{\partial y^2}-S_0\frac{\partial u}{\partial y}+g\beta(T-T_0)-\frac{\sigma\beta_0{}^2 u}{\rho}=0 \quad (3.2)$$

Energy Equation

$$u\frac{\partial T}{\partial y}+S_0\frac{\partial T}{\partial y}=\frac{k}{\rho CP}\frac{\partial^2 T}{\partial y^2}\frac{1}{\rho CP}\frac{\partial qr}{\partial y}+\frac{Q(T-T_0)}{\rho CP} \quad (3.3)$$

Together with the following boundary condition of interest

$$\left.\begin{aligned}
u(y=0)&=\frac{2-g_v}{g_v}\lambda\left.\frac{du}{dy}\right|_{y=0}\\
u(y=1)&=\frac{2-g_v}{g_v}\lambda\left.\frac{du}{dy}\right|_{y=1}\\
\theta(y=0)&=T_1+\frac{2-g_t}{g_t}\frac{2\gamma_s}{\gamma_s+1}\frac{k}{\mu CP}\lambda\left.\frac{dT}{dy}\right|_{y=0}\\
\theta(y=1)&=T_0+\frac{2-g_t}{g_t}\frac{2\gamma_s}{\gamma_s+1}\frac{k}{\mu CP}\lambda\left.\frac{dT}{dy}\right|_{y=1}
\end{aligned}\right\} \quad (3.4)$$

Following Zaheer *et al.*, (2020), the radiative heat flux is described by the Rosseland approximation, which gives the relation below:

$$q_r=\frac{-4\sigma^*}{3k^*}\frac{\partial T^4}{\partial y} \quad (3.5)$$

Where k^*,σ^* indicates the mean absorption coefficient and the Stefen-Boltzmann constant, by presumption that the temperature difference through the flow is small, the term T^4 expanded as a linear function of the temperature in Taylor's series about T_0 and neglecting the higher terms found that:

$$T^4\cong 4T_0^3T-3T_0^4 \quad (3.6)$$

Similarly, the dimensionless variables are explained below:

$$\left.\begin{aligned}
&Y=\frac{y}{b},U=\frac{u}{U_0},\theta=\frac{T-T_0}{T_1-T_0},S=\frac{Sob}{v},Ks=\frac{b^2Q}{u}\\
&\Pr=\frac{\mu CP}{u},\rho=\frac{\mu}{v},Ln=\frac{\beta_t}{\beta_v},Kn=\frac{\lambda}{b},U_0=\frac{\rho g\beta\left(T-T_0\right)b^2}{\mu}\\
&\beta_v=\frac{2-g_v}{g_v},\beta_t=\frac{2-g_t}{g_t},M^2=\frac{\sigma\beta_0{}^2b^2}{\rho v},Nr=\frac{1}{3kk^*}16\sigma^*T_0^3
\end{aligned}\right\} \quad (3.7)$$

The above dimensionless variables of equation (3.7) are transformed as below:

$$\left.\begin{aligned}
&Yb=y,\Rightarrow b\partial Y=\partial y,b^2\partial Y^2=\partial y^2\\
&UU_0=u,\Rightarrow U_0\partial U=\partial u,U_0\partial^2U=\partial^2u\\
&\left(T_1-T_0\right)\theta=T-T_0\Rightarrow\left(T_1-T_0\right)\partial\theta=\partial T,\\
&\left(T_1-T_0\right)\partial^2\theta=\partial^2T
\end{aligned}\right\} \quad (3.8)$$

Differentiating equation (3.5) to have

$$\frac{\partial q_r}{\partial y} = \frac{\partial}{\partial y}\left(-\frac{4\sigma^*}{3k^*}\frac{\partial T^4}{\partial y}\right) \quad (3.9)$$

Also differentiating equation (3.6), to have

$$\frac{\partial T^4}{\partial y} = 4T_0^{\,3}\frac{\partial T}{\partial y} \quad (3.10)$$

Substitute equation (3.10) into (3.9) to yield

$$\frac{\partial qr}{\partial y} = \frac{\partial}{\partial y}\left(\frac{-4\sigma^*}{3k^*}.4T_0^{\,3}\frac{\partial T}{\partial Y}\right) \quad (3.11)$$

Using equation (3.11) into equation (3.3), gives

$$U\frac{\partial T}{\partial y} + S_0\frac{\partial T}{\partial y} = \frac{k}{\rho CP}\frac{\partial^2 T}{\partial y^2} - \frac{1}{\rho CP}\frac{\partial}{\partial y}\left[\frac{-4\sigma^*}{3k^*}.4T_0^{\,3}\frac{\partial T}{\partial y}\right] + \frac{Q}{\rho CP}(T - T_0) \quad (3.12)$$

Substitute equations (3.7) into (3.2), (3.4), and (3.12) to have the dimensionless momentum equation, heat transfer equation, and corresponding dimensionless boundary conditions as:

Dimensionless Momentum Equation

$$\frac{d^2u}{dY^2} - S\frac{du}{dY} + \theta - M^2u = 0 \quad (3.13)$$

Heat Transfer Equation

$$(1+Nr)\frac{d^2\theta}{dY^2} - Spr\frac{d\theta}{dy} + Ks\theta = 0 \quad (3.14)$$

Dimensionless Boundary Conditions

$$\left.\begin{aligned} U(0) &= \beta_v kn \left.\frac{du}{dY}\right|_{y=0} \\ \theta(0) &= \mathrm{E} + \beta vKnLn\left.\frac{d\theta}{dY}\right|_{y=0} \end{aligned}\right\} \text{ at } Y = 0 \quad (3.15)$$

$$\left.\begin{aligned} U(1) &= -\beta vkn\left.\frac{du}{dY}\right|_{y=1} \\ \theta(1) &= 1 - \beta vknLn\left.\frac{d\theta}{dY}\right|_{y=1} \end{aligned}\right\} \text{ at } Y = 1 \quad (3.16)$$

3. METHOD 0F SOLUTION

Solving equations (3.13) and (3.14) using boundary conditions in equations (3.15) and (3.16), we obtain the velocity and temperature profiles as:

Velocity profile

$$U(y) = B_3e^{x_3y} + B_4e^{x_4y} + C_1e^{x_1y} + C_2e^{x_2y} \quad (3.17)$$

Temperature profile

$$\theta(y) = B_1e^{x_1y} + B_2e^{x_2y} \quad (3.18)$$

Differentiating equation (3.18) with respect to y to have

$$\frac{d\theta}{dY} = B_1 x_1 e^{x_1 y} + B_2 x_2 e^{x_2 y} \quad \ldots (3.19)$$

Equally, differentiating equation (3.17) with respect to y yields

$$\frac{dU}{dY} = B_3 x_3 e^{x_3 y} + B_4 x_4 e^{x_4 y} + C_1 x_1 e^{x_1 y} + C_2 x_2 e^{x_2 y} \quad \ldots (3.20)$$

In the presence of an applied magnetic field, the dimensionless form of the volumetric rate of entropy generation for a viscous fluid that conducts electricity is written as:

$$Ns = \left(\frac{\partial\theta}{\partial Y}\right)^2 + \frac{Br}{\Pi}\left(\frac{\partial U}{\partial Y}\right)^2 + \frac{Br}{\Pi} M^2 U^2 \quad \ldots (3.21)$$

Substitute the temperature solution of equation (3.18) and velocity equation (3.17) into equation (3.21) to have a dimensionless form of entropy generation as follows:

3.1 Entropy Generation

$$Ns = \left(B_1 x_1 e^{x_1 y} + B_2 x_2 e^{x_2 y}\right)^2 + \frac{Br}{\Pi}\left(B_3 x_3 e^{x_1 y} + B_4 x_4 e^{x_1 y} + C_1 x_1 e^{x_1 y} + C_2 x_2 e^{x_2 y}\right)^2 + \ldots$$
$$\frac{Br}{\Pi}.M^2\left(B_3 e^{x_3 y} + B_4 e^{x_4 y} + C_1 e^{x_1 y} + C_2 e^{x_2 y}\right) \quad \ldots (3.22)$$

3.2 Bejann Number

The Bejan number, which is another form of irreversibility, is given.

$$Be = \frac{\left(\frac{\partial\theta}{\partial Y}\right)^2}{\left(\frac{\partial\theta}{\partial Y}\right)^2 + \frac{Br}{\Pi}\left(\frac{\partial U}{\partial Y}\right)^2 + \frac{Br}{\Pi} M^2 U^2} \quad \ldots (3.23)$$

Substitute the temperature equation (3.18) and velocity equation (3.19) into (3.23) to have dimensionless of Bejan number as follows:

$$Be = \frac{\left(B_1 x_1 e^{x_1 y} + B_2 x_2 e^{x_2 y}\right)^2}{\left(B_1 x_1 e^{x_1 y} + B_2 x_2 e^{x_2 y}\right)^2 + \frac{Br}{\Pi}\left(B_3 x_3 e^{x_1 y} + B_4 x_4 e^{x_1 y} + C_1 x_1 e^{x_1 y} + C_2 x_2 e^{x_2 y}\right)^2 + \ldots} \quad \ldots (3.24)$$
$$\frac{Br}{\Pi}.M^2\left(B_3 e^{x_3 y} + B_4 e^{x_4 y} + C_1 e^{x_1 y} + C_2 e^{x_2 y}\right)$$

3.3 Skin Friction

Using the derivatives of velocity equation (3.17), the skin friction coefficient (τ) at $(y = 0, y = 1)$ resp. are as follows:

The skin friction coefficients for the upper and lower plates, respectively, are given as:

$$\tau_1 = \left.\frac{dU}{dY}\right|_{Y=1} = B_3 x_3 e^{x_3} + B_4 x_4 e^{x_4} + C_1 x_1 e^{x_1} + C_2 x_2 e^{x_2} \quad \ldots (3.25)$$

$$\tau_0 = \left.\frac{dU}{dY}\right|_{Y=0} = B_3 x_3 + B_4 x_4 + C_1 x_1 + C_2 x_2 \quad \ldots (3.26)$$

3.4 Volume Flow rate

The non-dimensional volume flow rate is given as adopted in the work of *Zaheer et al*., (2020)

$$Q = \frac{m}{bU_0} = \int_o^1 UdY \quad \text{……} (3.27)$$

Substitute equation (3.17) into (3.27) to obtain a dimensionless form of volume flow rate.

$$Q = \left(e^{x_3} - 1\right)\frac{B_3}{x_3} + \left(e^{x_4} - 1\right)\frac{B_4}{x_4} + \left(e^{x_1} - 1\right)\frac{C_1}{x_1} + \left(e^{x_2} - 1\right)\frac{C_2}{x_2} \quad \text{……} (3.28)$$

3.5 Heat Transfer rate

To have dimensionless form expressed by substituting the temperature equation (3.19) into the below relation:

$$Nu_0 = \left.\frac{d\theta}{dY}\right|_{y=0} = B_1 x_1 + B_2 x_2 \quad \text{……} (3.29)$$

$$Nu_1 = \left.\frac{d\theta}{dY}\right|_{y=1} = B_1 x_1 e^{x_1} + B_2 x_2 e^{x_2} \quad \text{……} (3.30)$$

4.0 RESULT AND DISCUSSION

The results of the current parametric analysis have been considered over a suitable range of $0 \le \ln \le 10$ and $0 \le \beta v Kn \le 0.1$ the quantity of separation from the continuum system and the property of the fluid wall interaction. The parametric value of suction or injection lies between $-2 \le S \le 2$ with reference value of, the thermal radiation is taken with a reference value of $Nr = 0.2$, the default value of the Prandtl number is $\Pr = 1.5$, porous material $K = 1.5$ and that of the heat source/sink is taken as $Ks = 2$. In order to have a good understanding of the effect of various controlling parameters on the flow formulation, a MATLAB (short for Matrix Laboratory) programme is written to compute and generate line graphs for the profiles mentioned.

Figures 4.2a and b represent velocity profiles for different values of fluid parameters.

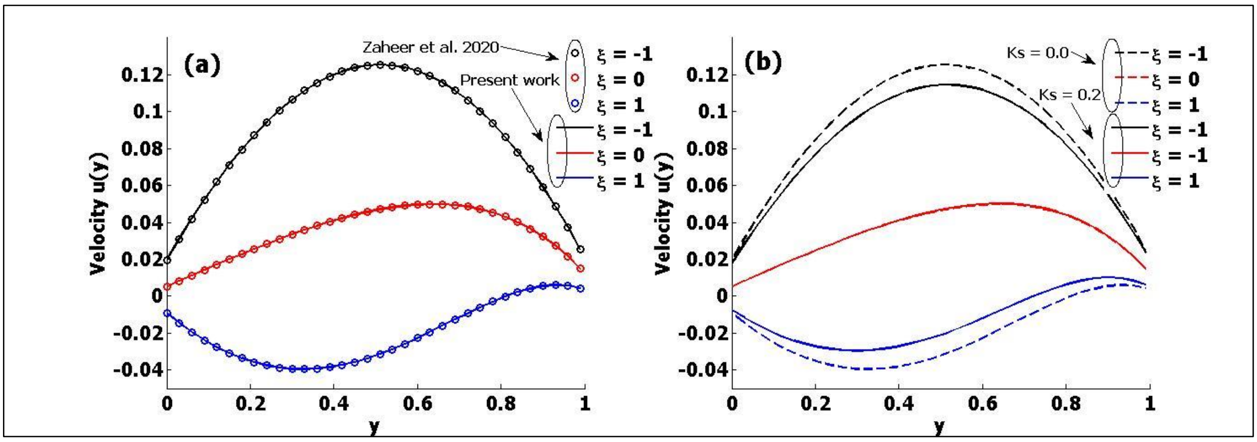

Figure 4.2a and b: Comparison between present work and that of Zaheer *et al.*, (2020) when $M = 1.5$, $S = 1$ and $Ks = 0.0$. And figure 4.2 b when $Ks = 0.2, \zeta = 1$.

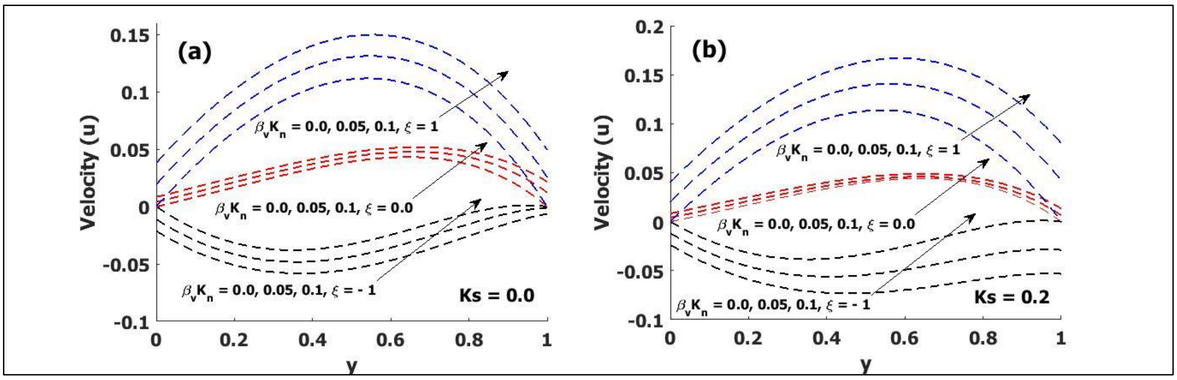

Figure 4.3a and b: Velocity profiles for the impact of $BvKn$ **when** $M = S = 1$ **at** $\xi = -1, 0, 1$

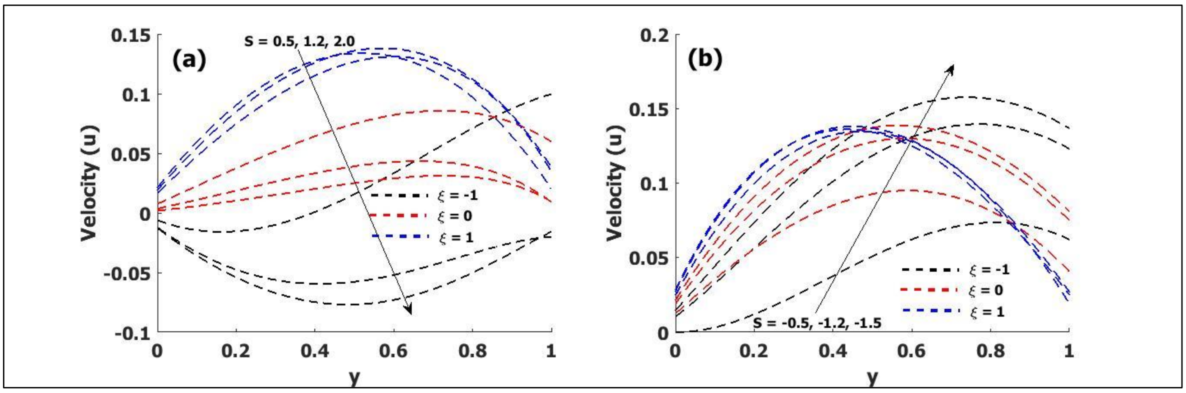

Figure 4.4a and b: Velocity profile for the impact of S **when** $M = 1$, **and** $Ks = 0.2, 0.4, 0.6$ **at fixed** $\xi = -1, 0, 1$.

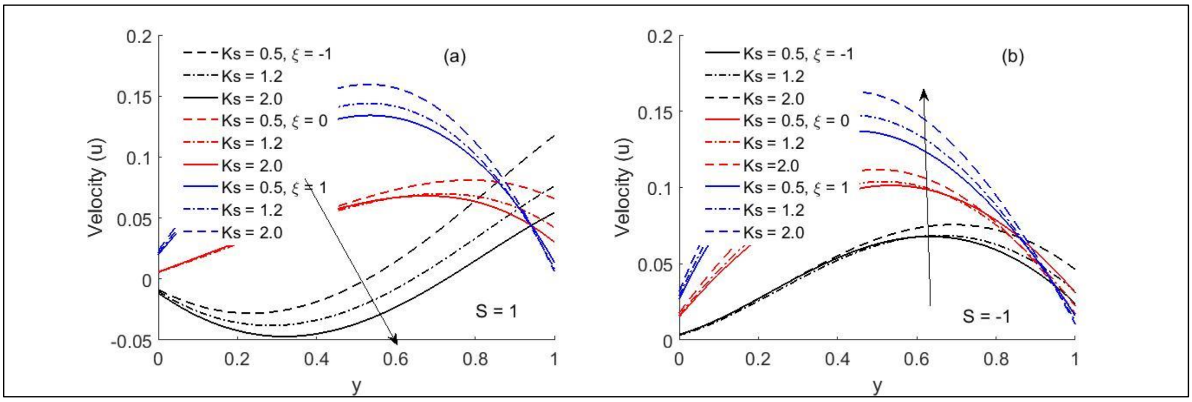

Figure 4.5a and b: Velocity profile for the impact of Heat source /sink Ks **when** $S = M = 1$ **at distinct values of** $\xi = -1, 0, 1$.

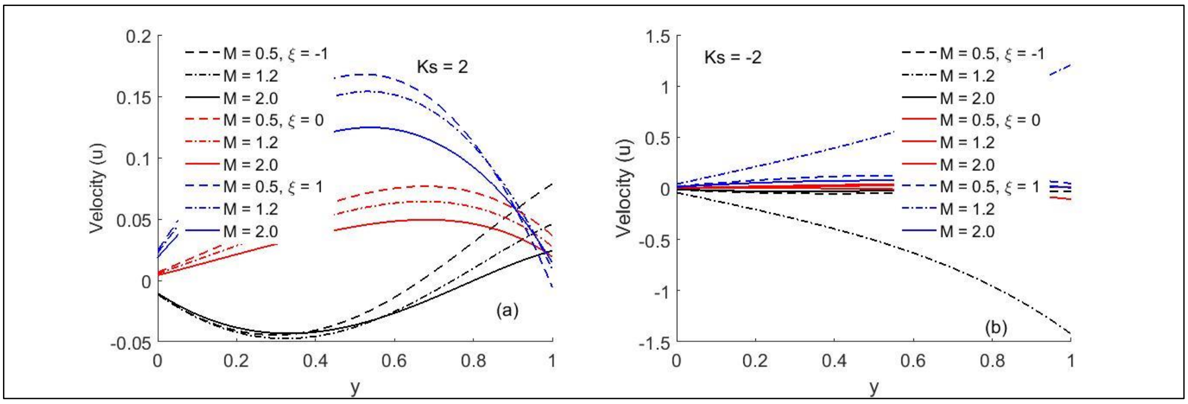

Figure 4.6a and b: Velocity profile for the impact of Magnetic parameter M **, fluid wall interaction parameter** $(\zeta = 0,1)$ **and Heat source/sink** $(K_s = 2, -2)$.

Temperature Profiles

The graph below shows the temperature profiles.

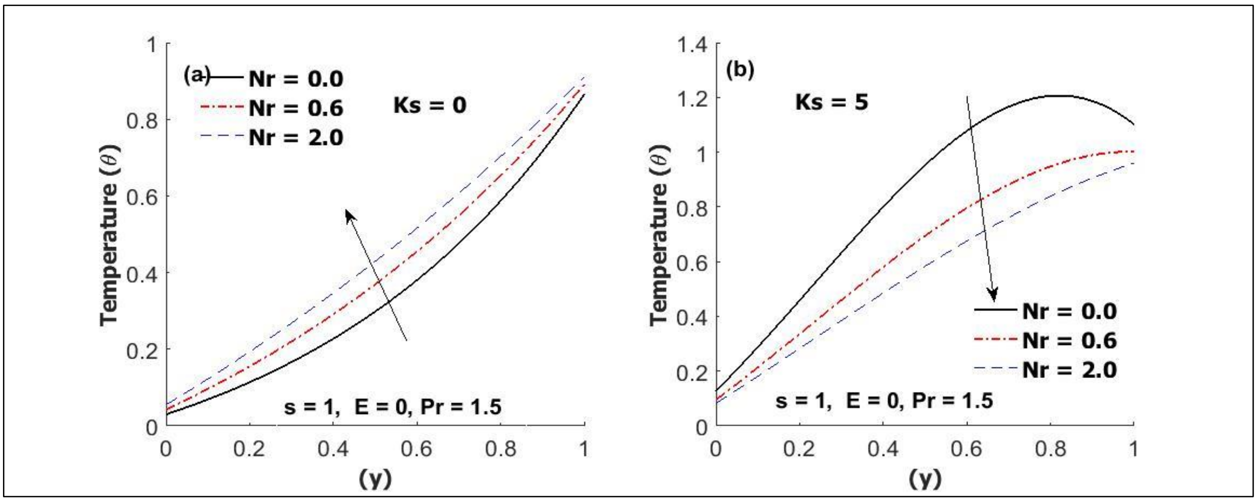

Figure 4.7a and b: Temperature profile for the impact of Heat source/Sink (K_s) when $S = 1, -1$ and $Nr = 0.2$

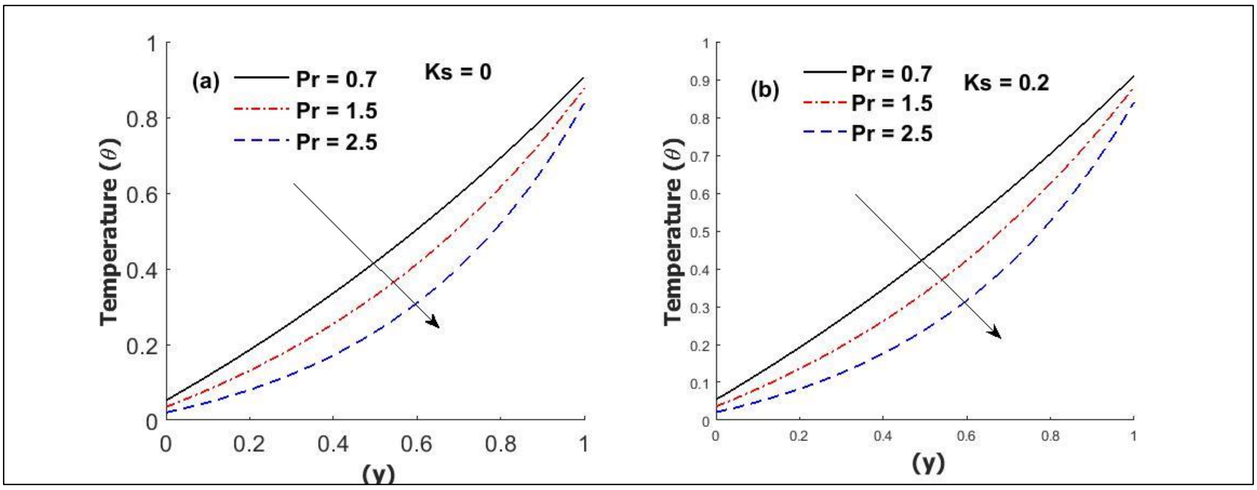

Figure 4.8a and b: Temperature profile for the impact of different values of the Prandtl number (P_r) against Ks .

The Skin friction profiles

Figures below present skin friction profiles.

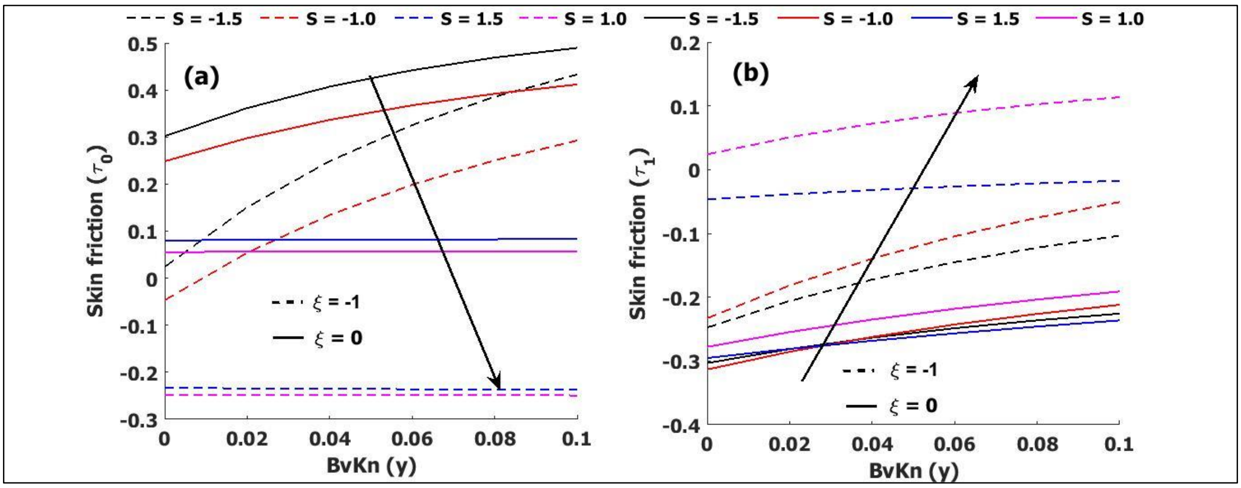

Figure 4.9a and b: Skin friction profile against $B_v K_n$ with varying effect of suction/injection

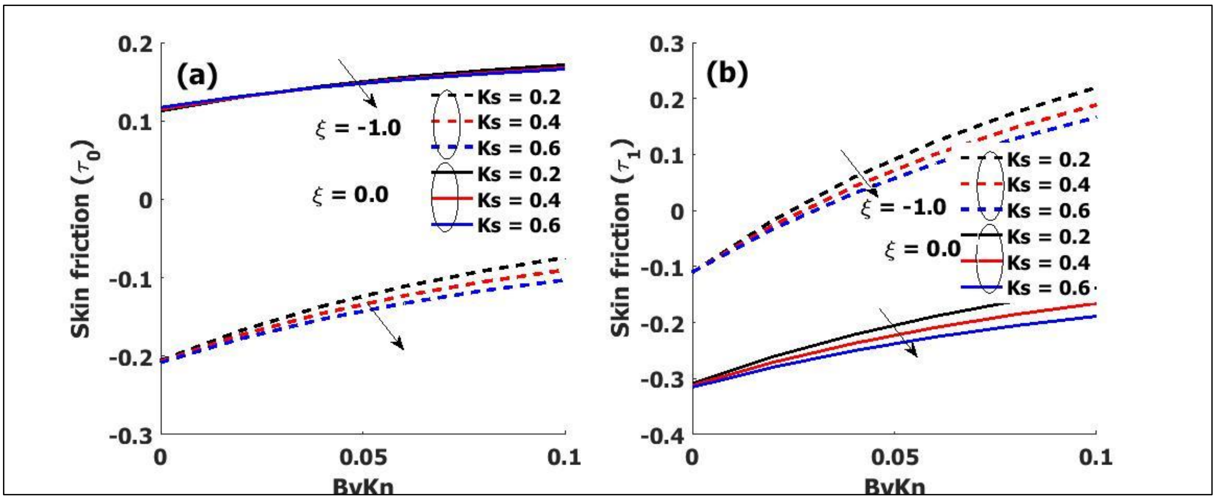

Figure 4.10a and b: The Skin friction profile against $B_v K_n$ with varying effect of Ks when $\zeta = -1, 0$

Volume Flow rate profiles

The volume flow rate profiles are shown in the figure below.

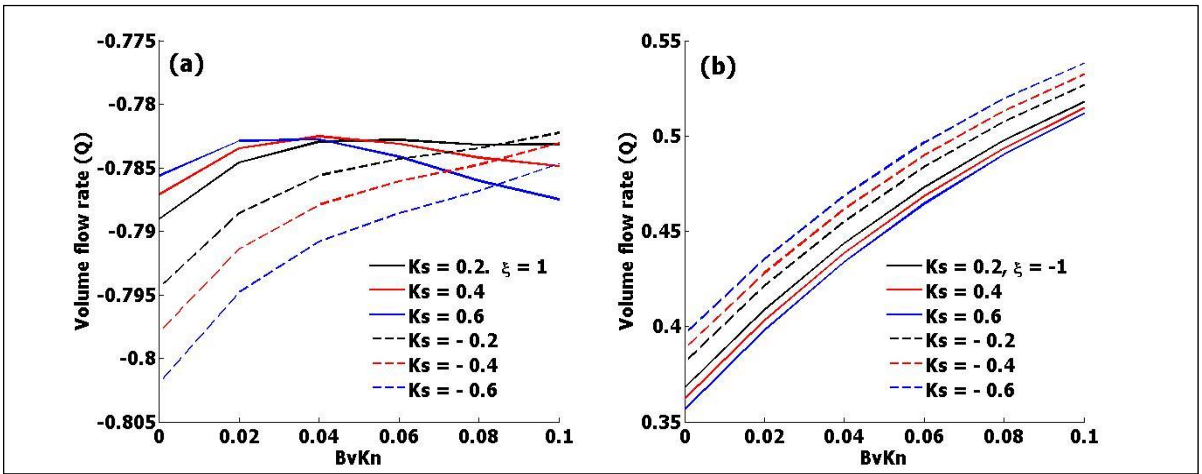

Figure 4.11a and b: Volume flow rate against $B_v K_n$ with varying effect of Ks at $\zeta = 1, -1$

Entropy Generation Profiles

The entropy generation profiles are depicted in the following figures:

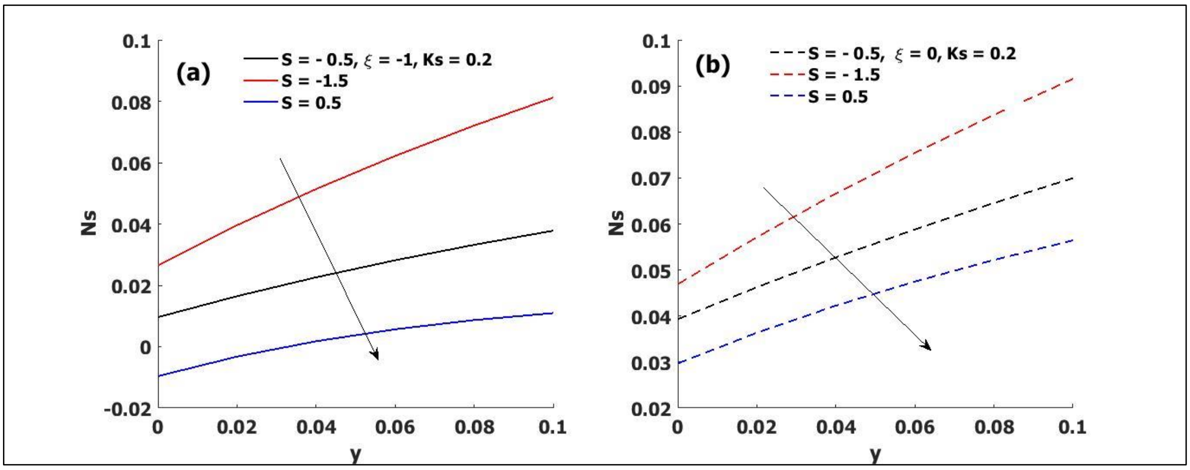

Figure 4.13a and b: The impact of suction /injection parameter on entropy generation with different values of (ζ) and Ks.

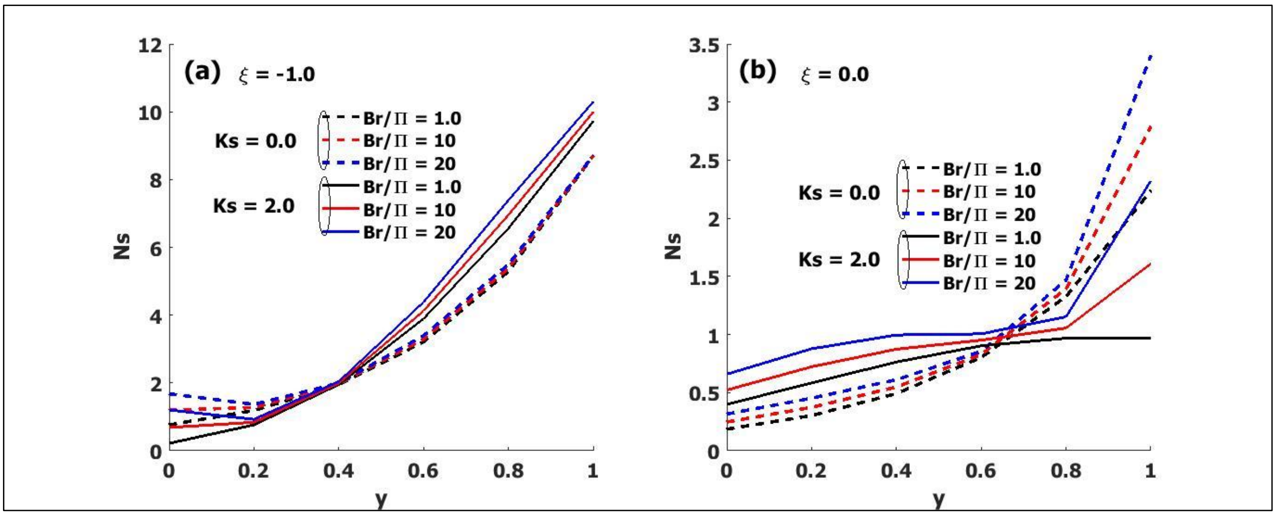

Figure 4.14a and b: Entropy generation with varying effect of Brickman's number with distinct values of ζ and Ks.

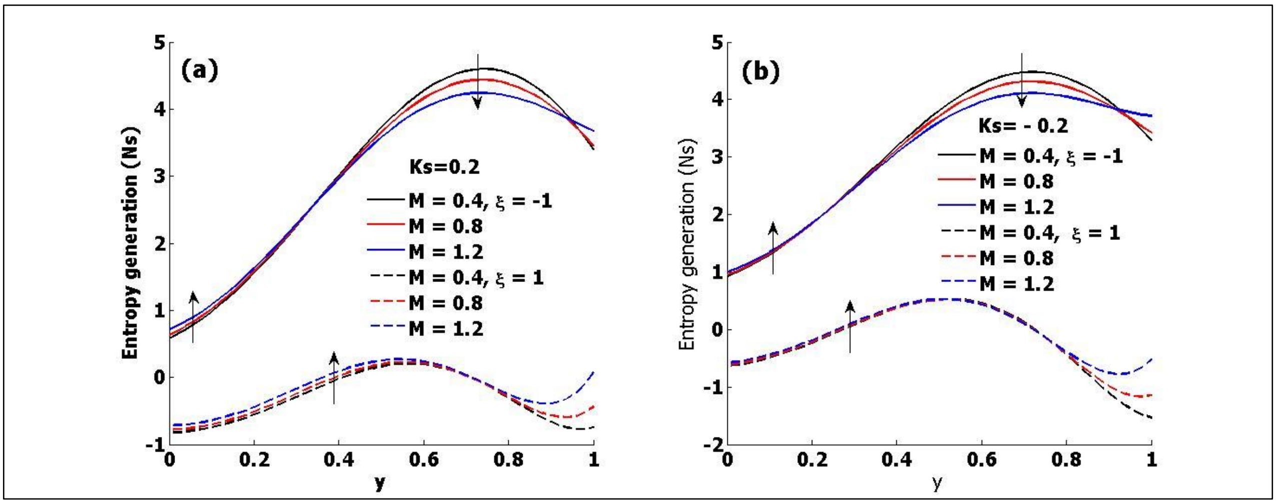

Figure 4.15a and b: Entropy profile with varying the effect of magnetic parameter M and Heat source Ks when $\zeta = 1, -1$.

Velocity Profiles

Figure 4.2a shows the comparison between Zaheer *et al.,* (2020) and the present work. From the figure, an excellent agreement was found, which ascertains the validity and accuracy of the present solution. In figure 4.2b, the velocity profile is remarkably appreciated without a heat source $(Ks = 0)$ in comparison with the presence of heat source $(Ks = 0.2)$ when temperature difference ratio is $(\zeta = -1)$ less than zero. Furthermore, a contrast phenomenon is observed when the fluid temperature difference ratio is $(\zeta = 1)$ greater than zero. In Figures 4.3a and b, the velocity increases with improving values of $B_v K_n$ and ζ. However, the result of velocity appears to be high $Ks = 0.2$ and $\zeta = 1$ as depicted in figure 4.3b.

The impact of the suction /injection parameter is demonstrated in figures 4.4a and b. In figure 4.4a, the velocity tends to decrease with high values of suction $(S > 0)$ and ambient fluid parameters with different ratios ζ. However, figure 4.4b reports the increasing behavior of velocity due to injection $(S < 0)$.

Figures 4.5a and b show the effect of the heat source on the velocity profile due to suction and injection. Figure 4.5a reveals that increasing the heat source parameter reduces velocity in the presence of suction $(S > 0)$. In the case of injection $(S < 0)$, the velocity increases with high values of the heat source parameter (Ks).

The contribution of magnetic number (M) on velocity is presented in figures 4.6a and b. Figure 4.6a demonstrates the effect of magnetic number (M) on velocity in the presence of a heat source $(Ks > 0)$. From the figure the values of velocity diminish with increasing values of M. In figure 4.6b, the suction $(Ks < 0)$ observed shows that increasing values of (M) lead to decreasing velocity.

Temperature Profile

Figures 4.7a and b present the effect of heat source /sink (Ks) on the temperature profile. It is obvious from figures 4.7a and b that temperature increases with an increase in the heat source with both suction/injections. $(S=1)$ However, in figure 4.7b, temperature is more clearly stated $(S<0)$. Figures 4.8a and b show the impact of different values of the Prandtl number (P_r). From the figures, the temperature profile decreases with increasing values of the Prandtl number, when $(Ks=0)$ but in figure4.8b temperature tends to keep increasing with $(Ks=0.2)$ in which also increases the Prandtl number.

Skin Friction

Figures 4.9a and b demonstrate the skin fiction against B_vK_n with distinct values of S. In figure 4.9a, skin friction reduces due to suction/injection at $y=0$ and increases at $y=1$. In figures 4.10a and b skin friction is plotted against B_vK_n with varying effects of Ks and ζ. From the figures, skin friction increases with increasing B_vK_n and decreases with Ks and ζ for both suction and injection. However, the skin friction values are high in the case of suction (see figure 4.10a) in comparison with injection, as reported in figure 4.10b.

Volume Flow rate

In Figure 4.11a and b, volume flow rate is demonstrated against (B_vK_n) with different values of (Ks) and ζ. In figure 4.11a, the volume flow rate moves up to high values of (B_vK_n) and Ks for the positive values of ambient fluid temperature difference ratio $(\zeta=1)$. However, in figure 4.11b, volume flow rate increases with (B_vK_n) and decrease with (Ks) when ambient fluid temperature different ratios assume negative values $(\zeta=-1)$.

Bejan number

In Figures 4.12a and b, describe the impact of the fluid-wall interaction parameter (Ln). It was observed that the Bejann number (Be) is decreasing with increasing values of the fluid-wall interaction parameter when $(\zeta=0,-1)$ and $(Ks=0)$ moves up to a point where $(y\simeq 0.7)$ it completely overlaps. It is observed in Figure 4.12b that the Bejan number increases with increasing values of the fluid wall interaction parameter $(\ln)$ from $(y=0)$ to $(y=0.3)$ it take reverse direction as $(y=0.32)$ to $(y\simeq 0.55)$ when twisted together at two values of $(\zeta=0,-1)$.

Entropy Generation

Figure 4.13a and b show that entropy generation decreases with the increase of the suction parameter (S) with higher values of heat source when $(\zeta=-1)$, while in Figure 4.13b also presents entropy generation profiles that decrease downward with the increase of the suction parameter due to the large value of the heat source at $(\zeta=0)$.

Figure 4.14a shows entropy generation increases with higher values of Brickman's number due to an increase in heat source at $(y=0.2)$ to $(y=0.4)$ the impact swings move upward. But in Figure 4.14b, the entropy generation increases with an increase in Brickman's number when $\zeta=-1$ between $0\le y\le 4$ and twists to decreases at $y=1$. However, the values of entropy generation appear to be high for $(Ks=0)$ from $(y=0.6)$ when $(Ks=2)$ as demonstrated in figure 4.14b.

Figure 4.15a and b show the impact of heat source (Ks) and magnetic number on the entropy generation. The variation of (M) increases entropy generation rate due to negative values of (ζ) but changes occur at a point when $(y=0.4)$ to take direction at $(y=0.6)$. It suddenly changes to its coincidental state; see figures 4.15a and b. While in both figures 4.15a and b the entropy increases with an increase (M) when (ζ) take positive values.

5.0 CONCLUSION

The study has investigated the hydrodynamics and thermal radiation flow of viscous fluid in a vertical porous channel due to a heat source/sink. The coupled system of differential equations with a constant coefficient governing the new formulated models was solved by the Method of Undetermined coefficient. To illustrate fluid flow behaviour and the impact of each varying parameter for velocity, temperature, and skin friction, a volume flow rate time graph was plotted using the MATLAB package. The following conclusions were drawn:

1. The values of velocity are higher when $Ks=0$ and $\zeta=-1$ as showed in figure 4.2b, velocity tends to decrease due to injection $(S>1)$. However, the values of velocity in contrast are observe from the same figure when $Ks=0.2, \zeta=1$ respectively.
2. The effect of heat source (Ks) on velocity revealed that velocity decreases at higher values

of $(S=1)$ due to increases in heat source. But it is clearly seen that velocity increases with decreasing values of (Ks) when suction $(S=-1)$ for all values of $(\zeta=0,-1,1)$.

3. Present the effect of heat source /sink (Ks) on the temperature profile. It is obvious from the figures that temperature increases with an increase in heat source with both suction/injection $(S=1)$ and radiation parameter $(N_r=0.2)$.
4. Skin friction increases with increasing $B_v K_n$ and decreases with Ks and ζ for both suction and injection.
5. Volume flow rate appreciated with positive values of heat source (Ks) for some values of $(B_v K_n)$ 0 to 0.04 and experience twist from 0.04 to 0.1. However, the values of volume flow rate decrease with decreasing values of heat sink (Ks).
6. The Bejan number (Be) it is noticed to be decreased with increases of $(\ln)$ and $(\zeta=0,-1)$ when heat source $(Ks=0)$ around the point$(y\simeq 0.7)$. However, it was observed that the Bejan number increased with an increase in whilst $(\ln)$ parameter from $(y=0)$ to $(y=0.3)$ but took the reverse direction by decreasing from$(y\simeq 0.32)$ to $(y\simeq 0.56)$ then after slap together.
7. Entropy generation it is evident that entropy generation increases with higher values of $\left(\frac{B_r}{\Pi}\right)$ when $(Ks=0)$. However, for $(Ks=0.2)$ the distinct values of Brickman's number, interchange the radiation parameter at different ranges of (y) the (N_s) decrease with an increase in $\left(\frac{B_r}{\Pi}\right)$ at $(y=0.3)$ swing to increase and suddenly begin to fall at $(y=0.8)$.

NOMENCLATURE

Symbol	Description
b	Channel width
B_0	Constant magnetic field
C_p	Specific heat at constant pressure
C_v	Specific heat at constant volume
g_t	Thermal momentum accommodation coefficient
g_v	Tangential momentum accommodation coefficient
g	Gravitational acceleration
In	Fluid-wall interaction parameter
Kn	Knudsen number
m	Volume flow rate
Q	Dimensionless volume flow rate
Nu	Dimensionless heat transfer rate(Nusselt number)
$\Pr$	Prandtl number
Ec	Eckert number
S	Suction/injection parameter
Nr	Radiation parameter
T	Temperature of fluid
T_0	Reference temperature
u, v	Velocity components in x, y direction
U	Dimensionless velocity
S_0	Constant suction/injection velocity
B_e	Bejan number
$\frac{B_r}{\pi}$	Brinkman number,= $Er\Pr$
N_s	Entropy generation number
M	Hartmann number
Υ_s	Ratio of specific heat
Greek Symbol	
σ	Electrical conductivity
ℓ	Density
λ	Molecular mean free path
β	Thermal expansion coefficient
µ	Dynamic viscosity
σ^*	Stefan-Boltzmann constant
k^*	Mean absorption coefficient
θ	Incline angle

REFERENCES

- Amoo, S. A., & Idowu, A. S. (2017). Thermal radiation effects on heat and mass transfer of MHD flow in porous media over an exponentially stretching surface. *FUW Trends in Science & Technology Journal Nigeria*, *2*(1), 33-41.
- Bhattacharya, K. (2011). Effect of radiation and heat source/sink on unsteady MHD boundary layer flow over a shrinking sheet with suction /injunction. *Front. Chemical Science Engineering*, *5*, 376-384.
- Barmert, G., & Kupitz, J. (1991). World Energy Council: *90 Years of Energy Coporation, Report*, 1923-2013, p 13.

- Bhuvaneswari, M., Sivasankaraan S., & Kim, Y. J. (2010). Exact analysis of radiation convective flow heat and mass transfer over an inclined plate in a porous medium, *World Applied Science Jounal*, 10, 774-778.
- Biddend, B., & Nazar, R. (2009). Numerical solution of the boundary layer flow over an exponentially stretching sheet with thermal radiation, *European Journal Science Resource, 33*(4), 710-717.
- Barik, R. N., Dash, G. C., & Rath, P. K. (2014). Thermal radiation effect on an unsteady MHD flow past inclined porous heated plate in the presence of chemical reaction and viscous dissipation. *Applied Mathematics Computation,* 226(1), 423-434.
- Bejan, A. (1982). Second-law analysis in heat transfer and thermal design. *Advance Heat Transfer International Article*, 15, 1-56.
- Bejan, A. (1995). The science and the History of two Bejan numbers. *International journal Heat and Mass Transfer, 37*(8), 1283.
- Batti, M. M., Rashidi, M. M., & Pop. (2017). Entropy generation with nonlinear heat and mass transfer on MHD Boundary layer over a moving Surface. *De Gruyter nonlinear Engineering, 6*(1), 43- 48.
- Chen, T. S., & Moutsoglou, A. (1980). A Combined Heat and Mass Transfer in Mixed Convection along a vertical and inclined plate, *International Journal Heat and Mass Transfer*, 23, 527-537.
- Erickson, L. E., & Cha L. T. (1966). Fan the cooling of moving continuous flat sheet, *AICHE Journal*, 62, 157-165.
- Farhad, A., Anees, I., Waqar, A. K., Ilyas, I., & Irfan B. (2020). Effect of MHD and porosity on entropy generation in two-dimensional, Newtonian fluid over a thin needle, *Scientific Report a parallel Stream*, 10, 223-235.
- Hooman, K. (2008). Heat transfer and entropy generation for forced convection through a micro duct of rectangular cross section effect of velocity slip, temperature jump and duct geometry. *International common Heat Mass Transfer Journal*, 35, 1065-1068.
- Isah, B. Y., Altine, M. M., & Ahmad, S. K. (2019). Thermal Radiation and Variable pressure effect on natural convective Heat and Mass Transfer fluid flow porous medium, *Nigerian Journal of Basic Science*, *27*(1), 48-58.
- Jian, Y. (2015). Transient MHD heat Transfer and entropy generation in a micro parallel channel combined pressure and electro osmotic effects. *International Journal of Innovative Heat Mass Transfer,* 89, 193-205.
- John, D., & Emeka, A. (2020). MHD Free convection Heat and Mass Transfer Flow in a porous medium with Dufour and chemical reaction, *International Journal of Innovative Scientific Engineering Technology Research, 8*(2), 1-12.
- Jery, A. E., Hidouri, N., Magherbi, M., & Benbrahim, A. (2010). Effect of an external oriented magnetic field on entropy generation with nonlinear heat and mass transfer on MHD Boundary layer over a moving surface. *DE Gruyter nonlinear engineering*, *6*(1), 43-52.
- Kumar, J. P., Uwavathi, J. C., Chamkha, A. J., & Pop, I. (2017). Fully developed free convective flow of micro polar and viscous fluids in a vertical channel. *Applied Mathematical Model*, 34(5), 1175-1186.
- Lopez, A., Ibanez, G., Pantoja J., & Mareira, J. (2017). Entropy generation analysis of MHD fluid flow in porous vertical micro channel with nonlinear thermal radiation, slip flow and convective radiative boundary condition, *International Journal Heat and Mass Transfer,*107, 982-994.
- Madhusudhana, R. B., Viswanatha, G. R., & Raju, M. C. (2017). Thermal Radiation and Heat Transfer effect on the steady MHD fluid flow past a vertical porous with injection, *American-Eurasian Journal of Scientific Research*, *12*(4), 180-188.
- Makinde, O. D., & Mhone Y. P. (2005). Heat Transfer to MHD oscillatory flow in a channel filled with porous medium. *Rom journal of physics, 50*(10), 931-938.
- Mahmoudi, Y. (2015). Constant wall Heat flux boundary condition in micro-channel filled with porous channel with internal heat generation under local thermal non equilibrium condition. *International Journal of Heat Transfer* 85:524-542.
- Mukhopadhyay, S., Layek G. C., & Samd, S. A. (2011). Effect of variable fluid viscosity on flow past a heated scratching sheet embedded in porous medium in presence of heat source/sink. *Meccanica*, 47, 863-876.
- Mohamed, A., & Aisha, S. Y. (2017). Heat and Mass Transfer of unsteady hydromagnetic free convection flow through porous medium past a vertical plate with uniform surface heat flix. *Journal of Theoretical and Applied Mechaincs, Sofia, 47*(3), 25-58.
- Mahmud, S., & Fraser, R. A. (2005). Flow Heat flow on thermal radiation and entropy generation characteristic inside a porous channel with viscous dissipation. *International Journal thermal Science*, 44, 21-32.
- Manga Thai, P., Reddy, G., & Red, R. (2016). MHD free convective flow past a vertical porous plate in the presence s of radiation and heat generation. *Physics International journal of chemical Sciences.*
- Nasiri, M., Rashidi, M. M., & Lorenzini, G. (2015). Effect of Magnetic field on entropy generation in a micro channel heat sink with offset fan shaped, *International Journal of Heat Mass Transfer*, 1, 17.
- Ozisik, M. N. (1985). Heat Transfer, *McCrow-Hill: New York, Ny. USA.*
- Omowaye, A. J., Fagbade, A. I., & Ajayi, A. O. (2015).Dufour and Soret effect on Steady MHD

convective flow of a fluid in a porous medium with temperature dependent viscosity analysis approach, *Journal of the Nigerian Mathematical Society*, 34, 343-360.

- Rajakmark, U. B., Balamurugan, K. S., Reddly, M. U., & Ramana, V. M. (2018). Radiation Dissipation and Dufour on MHD free convective Casson fluid flow through a Vertical Oscillatory porous plate with Ion-ship Current. *Journal of Effect Ans Technology, 36*(2), 494-508.
- Saddek, M. A., & Salama, F. A. (2007). The effect of temperature dependent viscosity and thermal conductivity on unsteady MHD convective heat transfer past a semi -infinite vertical porous moving plate with variable suction. *Computed Mater Science, 40*(2), 186-192.
- Sanker, M. (2016). Mathematical Modelling of Moving through a fluid. *Fluid Dynamic* (pp (423-443).
- Sakiadis, B. C. (1961). Boundary layer behavior on continuous solid surface alongside equation of two dimensional and axisymmetric flow. *AICHE Journal*, 7, 26-28.
- Tasnim, S. H., Shohel, M., & Mamun, M. A. (2002). Entropy generation in a porous channel with hydromagnetic effect. *Exergy International Journal*, 2, 300-308.
- Uwanta, I. J., & Isah, B. Y. (2012). Boundary layer fluid flow in a channel with Source, Soret effect and Slip condition. *Nigerian Journal of Basic and Applied Sciences, 20*(4), 327-340.
- Usman, H., & Uwanta, I. J. (2013). Effect of thermal condition on MHD heat and Mass Transfer flow past and infinite vertical plate with Soret and Dufour effect. *American Journal of Applied Mathematics, 1*(3), 28-38.
- Verma, V. K., & Singh, S. K. (2015). Magnetohydrodynamic flow with varying viscosity in an annular channel. *Advance Theory of Applied Mathematics*, pp 105-122.
- Venkata Ramana, R. G., Ramana Murthy, C. V., & Bhaskar, R. N. (2010). Effect of critical parameters on MHD flow in a porous channel when suction decreases exponentially, *International Journal of Emerging Technology and Engineering Technology Sciences, 3*(2), 135-139.
- Zaheer, A., Muhammad, N., Meriyem, N., & Nadeem, S. (2020). Analysis of entropy generation for MHD flow of viscous fluid embedded in a vertical porous channel with thermal radiation, *Alexendria engineering Journal*, 59, 3395-3405.
- Zahmtkesh, R., Mohammadium, M., Mohammadium, M. H. D., & Bonab. (2019). Investigation of entropy generation in axisymmetric stagnation flow over a cylinder with constant wall temperature and uniform surface suction-blowing. *Alex Engineering Journal*, 58, 1483-1498.